

# Fast and Scalable Position-Based Layout Synthesis

Tomer Weiss, Alan Litteneker, Noah Duncan, Masaki Nakada, Chenfanfu Jiang,  
Lap-Fai Yu, *Member, IEEE*, and Demetri Terzopoulos, *Fellow, IEEE*

**Abstract**—The arrangement of objects into a layout can be challenging for non-experts, as is affirmed by the existence of interior design professionals. Recent research into the automation of this task has yielded methods that can synthesize layouts of objects respecting aesthetic and functional constraints that are non-linear and competing. These methods usually adopt a stochastic optimization scheme, which samples from different layout configurations, a process that is slow and inefficient. We introduce a physics-motivated, continuous layout synthesis technique, which results in a significant gain in speed and is readily scalable. We demonstrate our method on a variety of examples and show that it achieves results similar to conventional layout synthesis based on Markov chain Monte Carlo (MCMC) state-search, but is faster by at least an order of magnitude and can handle layouts of unprecedented size as well as tightly-packed layouts that can overwhelm MCMC.

**Index Terms**—Automatic layout synthesis; 3D scene modeling; Automatic content creation; Position-based methods; Constraints

## 1 INTRODUCTION

THE arrangement of objects into a desirable layout is an everyday problem that is nonetheless surprisingly complex. For example, to find a desirable furniture arrangement for a living-room, one must consider the visibility of the television, a suitable separation of sofas, and access to adjacent rooms, among other factors that differ according to taste and style. It is often difficult for people to solve layout problems, as is affirmed by the existence of professional interior layout designers and self-help resources.

The principal motivation in computer graphics for automatic or semi-automatic layout synthesis is the need to model realistic virtual worlds [1]. Methods that can automatically synthesize realistic, large-scale virtual environments (Fig. 1) are useful for gaming, educational, and training purposes. Such methods are more useful in practice if they can generate larger, more complex environments and execute faster.

In recent years, researchers have proposed several methods for synthesizing layouts that pose layout synthesis as a highly non-convex optimization problem subject to numerous constraints. Due to the challenging nature of these problems, previous work applied stochastic optimization to sample viable layout candidates. Markov chain Monte Carlo (MCMC) methods [2] are the preferred technique because the constraints are often difficult to express as differentiable functions. Unfortunately, these techniques become inefficient when dealing with large numbers of objects.

To overcome this problem, we introduce a continuous framework for layout synthesis. Our main observation is that there are commonalities between layout synthesis and



Fig. 1: A tightly-packed picnic layout (top), and a theater layout with a large number of chairs (bottom), automatically placed by our method given user-specified constraints that include distance, viewing angle, and spaciousness criteria.

- T. Weiss, A. Litteneker, M. Nakada, and D. Terzopoulos are with the University of California, Los Angeles.
- N. Duncan is with WorkPatterns, Inc.
- C. Jiang is with the University of Pennsylvania.
- L.-F. Yu is with the University of Massachusetts, Boston.

Manuscript received ?? ??, 2018; revised ?? ??, 2018.

the elastic simulation of deformable objects. Elasticity penalizes the deformation of an object—the energy increases proportionally to the magnitude of the deformation—and layout synthesis penalizes the magnitude of constraint violation. Both can be formulated as optimization problems,



Fig. 2: Tightly-packed picnic layouts (comprised of various numbers of different object types) synthesized by our method.

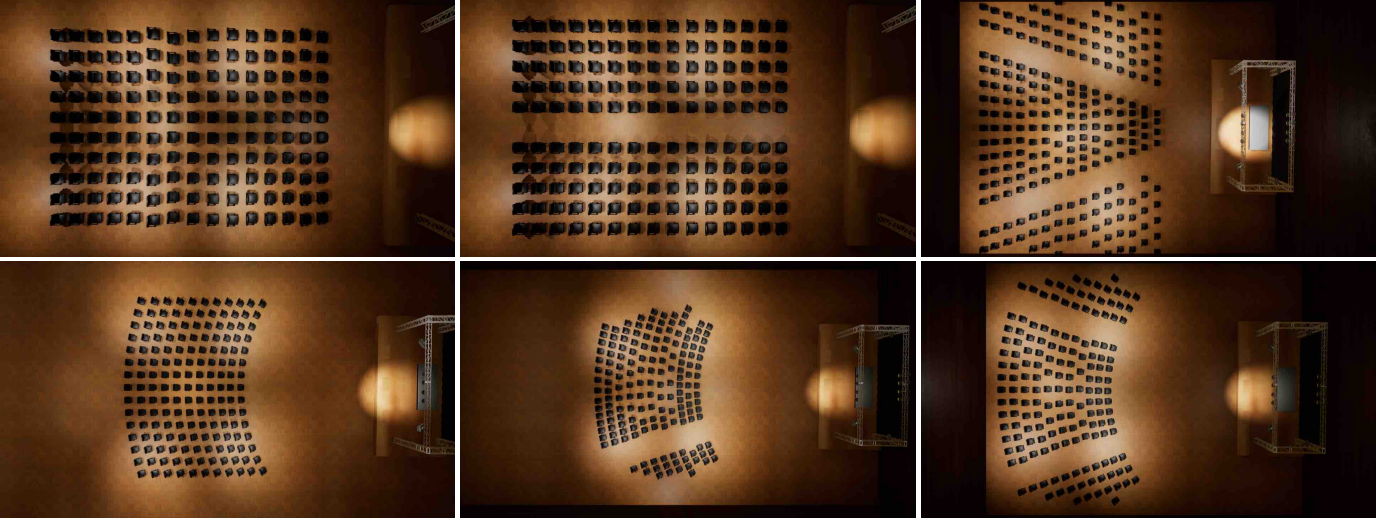


Fig. 3: Variations of the theater scenes synthesized by our method.

and both can be tackled using continuous optimization procedures. Our new, continuous approach enables the fast generation of large-scale, tightly-packed layouts that are intractable using previous approaches. However, like stochastic methods, our deterministic approach can synthesize multiple viable layouts for a given environment (Fig. 2, Fig. 3). To our knowledge, ours is the first physics-motivated approach to layout synthesis.

Our method takes as input an environment, a set of objects, and prescribed aesthetic and/or functional layout constraints that can be easily modified. Initially the positions and orientations of the objects are randomized, which is analogous to choosing a random initial guess in an iterative solver. Object positions and orientations are iteratively modified to achieve a viable layout. At each iteration, the objects are moved so as to satisfy competing constraints. Hard constraints such as observing layout boundaries and preventing collisions between layout objects are enforced by default. The procedure converges when all the prescribed constraints are adequately satisfied. We show that a diverse set of constraints, which have been applied in prior layout synthesis schemes, can be formulated within our framework. Layout objects can also be grouped, and each group assigned aesthetic or functional layout constraints. Groups are reusable in defining other layout groups, and they are also easily modifiable both in terms of the participating objects and the group layout constraints.

Our main contributions in this paper are as follows:

- 1) We propose a novel, physics-motivated approach to layout synthesis.
- 2) We formulate a set of common layout constraints within our framework.
- 3) We develop a novel, continuous and deterministic layout synthesis algorithm with significantly reduced computational cost, making large-scale layout synthesis problems tractable.

The remainder of the paper is organized as follows: Section 2 reviews relevant prior work. Section 3 presents the technical details of our approach. Section 4 describes our experiments and presents our results. In Section 5, we further discuss our framework, including its strengths and limitations, and suggest avenues for future work.

## 2 RELATED WORK

### 2.1 Layout Synthesis

We focus on layout synthesis problems in which a set of objects is to be arranged in an open space. The objects are assumed to be rigid bodies. The goal of the layout problem is to position and orient the objects such that they satisfy several functional and aesthetic criteria. These criteria are encoded as the terms of a non-convex objective function. The main challenge stems from finding an arrangement that respects conflicting terms, resulting in a multitude of possible layout outcomes, some of which may be unsatisfactory. Relevant publications in this category include the following:

Yu *et al.* [3] and Merrell *et al.* [4] introduced an McMC-based approach to furniture arrangement. Yeh *et al.* [5] formulated layout constraints with factor graphs, allowing a variable number of elements in the synthesized layout. These McMC-based, stochastic sampling methods can synthesize scenes that respect a complex and conflicting set of constraints, but they have been shown to work only on layouts with a limited number of objects and relaxed spacing. The underlying inefficiency of these approaches stems from the fact that they do not employ local gradient information—they merely sample a new position of a furniture item by applying a shift move to the current position.

Fu *et al.* [6] synthesize layouts from object relation graphs learned from a database of floor plans. Feng *et al.* [7] optimized mid-scale layouts by stochastically optimizing an objective function derived from agent-based simulation. Fisher *et al.* [8] generated small, local layouts of objects in a scene, guided by exemplars—e.g., the layout of items on a desk. Layouts are generated by sampling probabilistically from an occurrence model distribution. Additionally, the authors report that since the layout generation is probabilistic, it cannot handle hard constraints such as rigid grid layouts or exact alignment relationships.

Peng *et al.* [9] introduced a method that creates layouts from deformable templates, which differs from prior work that assumed objects are rigid. They incorporated a continuous method in their approach, but use it only to deform objects, whereas we use ours to position objects. Recently, Wu *et al.* [10] proposed a mixed integer-linear programming formulation for floor plan synthesis.

Layout research has also addressed contexts other than interior design. Majerowicz *et al.* [11] focused on adding objects to shelves in a 2D setting. Bao *et al.* [12] uses a combined stochastic and numerical optimization approach to explore and refine building layouts. Zhu *et al.* [13] synthesized layouts of mechanical components to control the motion of a toy. Cao *et al.* [14], [15] synthesized manga layouts. Reinert *et al.* [16] introduced an interactive layout generation method of arranging shapes according to aesthetic attributes, such as color and size. We focus on interior and exterior design layouts, but our method generalizes to other contexts.

## 2.2 Physics-Based vs Position-Based Methods

Physics-based modeling techniques have been used in various contexts, from animation [17], [18], to geometric design [19], [20], to architectural floor plan design [21], [22]. Position-Based Dynamics (PBD), independently introduced by Muller *et al.* [23] and by Stam [24], was originally proposed as a means of simulating physical models in situations, such as games, where speed and robustness takes priority over physical realism. Researchers have since applied the approach to a variety of simulations, from soft and rigid bodies [25], fluids [26], to crowd simulation [27]. PBD is part of a larger family of simulation methods called position-based methods. Bender *et al.* [28] present a survey. The common characteristic of these methods is that they work directly with positions rather than with forces as does true Newtonian dynamics (so PBD should more properly be called Position-Based Kinematics). The method works

---

### Algorithm 1

---

```

1: for Object  $i$  do
2:   Initialize  $\mathbf{p}_i = \mathbf{p}_i^0$ ;  $\theta_i = \theta_i^0$ 
3: Set  $l = 1$ 
4: while SolverIteration  $l < \max$  do
5:   UpdateStiffnesses( $C_1, \dots, C_m$ )
6:   ProjectConstraints( $C_1, \dots, C_m$ )
7:   for Object  $i$  do
8:     GenerateCollisionConstraints()
9:   ProjectCollisionConstraints()

```

---

by iteratively adjusting particle positions to satisfy a set of constraints. To our knowledge, we are the first to pursue this approach in the context of layout synthesis.

## 3 ALGORITHM

Starting from random initial layouts, our method explores sequences of possible object arrangements by iteratively solving user-prescribed layout constraints.

A layout is represented by a set of  $n$  oriented particles, each of which denotes the position and orientation of an associated 3D object mesh. Each particle  $i$  has three attributes:

- 1) a position  $\mathbf{p}_i$ ,
- 2) an orientation  $\theta_i$ , and
- 3) a mass  $m_i$ , and corresponding inverse mass  $w_i = 1/m_i$ , determined by the volume of the bounding box of the associated object.

Our algorithm modifies the position and orientation of each particle in order to satisfy a set of  $m$  layout constraints, which restrict the positions and orientations of several layout items. A constraint comprises

- a scalar constraint function  $C$ ,
- a stiffness parameter  $k \in [0, 1]$ , and
- a constraint type,

either an *equality* constraint  $C(\mathbf{p}) = 0$  or an *inequality* constraint  $C(\mathbf{p}) \geq 0$ , where  $\mathbf{p} = [\mathbf{p}_1^T, \theta_1, \dots, \mathbf{p}_n^T, \theta_n]^T$ .

Starting from a uniformly distributed random initial position for each object in the layout, our algorithm solves each constraint independently. The constraint’s spring-like stiffness determines the magnitude of the positional correction toward satisfying the constraint. The positional corrections are either processed sequentially, or averaged in a batch.

To measure the quality of a layout, we employ the energy function

$$E = \left( \sum_{j=1}^m \gamma_j C_j^2 \right)^{1/2}, \quad (1)$$

where  $C_j$  denotes constraint  $j$  with respective weight  $\gamma_j$ .

Algorithm 1 overviews our method. Line 2 initializes object  $i$  to a random location  $\mathbf{p}_i^0$  and orientation  $\theta_i^0$ . In each iteration of the main loop, starting at Line 4, each constraint  $C_i$  is calculated and immediately projected, so that the next constraint uses the updated result (details in Section 3.3). Collision constraints require special treatment, since they may change in each iteration, and are generated in Line 8 using a spatial hash (details in Section 3.3.9).

Each constraint  $C_i$  has an associated stiffness parameter  $k_i$  which is updated in each iteration (Line 5). Depending on

the constraint type, the stiffness either decreases, increases or remains constant. For example, the pairwise distance constraint decreases over time, the collision constraint increases, and for hard constraints, like the layout boundary, the stiffness is constant. This is a type of numerical continuation method [29]. Increasing the number of iterations results in more physically-plausible solutions. In addition, since some constraints are conflicting, we evaluate them in different orders, by interleaving them, similar to Stam’s proposal [24].

### 3.1 Constraint Projection

PBD satisfies a system of constraints by iteratively solving each constraint independently. According to Bender et al. [28], the correction  $\Delta \mathbf{p}$  is derived using the first-order approximation  $0 = C(\mathbf{p} + \Delta \mathbf{p}) \approx C(\mathbf{p}) + \nabla_{\mathbf{p}} C(\mathbf{p}) \cdot \Delta \mathbf{p}$  and restricting the correction to be in the direction of the constraint gradient: i.e.,  $\Delta \mathbf{p} = \lambda \nabla_{\mathbf{p}} C(\mathbf{p})$ . This leads to the following formula for the positional correction to particle  $i$ :

$$\Delta \mathbf{p}_i = -s \nabla_{\mathbf{p}_i} C(\mathbf{p}), \quad (2)$$

with scale factor

$$s = \frac{k w_i C(\mathbf{p})}{\sum_{i=1}^n w_i \|\nabla_{\mathbf{p}_i} C(\mathbf{p})\|^2}, \quad (3)$$

where the stiffness parameter  $k$  determines the influence of the constraint. The stiffness  $k^l$  at each iteration  $l$  varies according to  $k^l = 1 - (1 - k^0)^{M/l}$ , where  $k^0$  is the initial stiffness and  $M \geq 1$  determines the rate at which  $k^l$  approaches zero.

We employ two different schemes for satisfying constraints. Each constraint is either solved independently and projected, the updated particle position  $\mathbf{p}_i$  immediately becoming visible to other constraints, or a subset of constraints is solved as a batch. In the batch case, we average the positional corrections of all the constraints affecting  $\mathbf{p}_i$ , with averaging coefficient 1.2, as suggested by Macklin et al. [30].

A formula similar to (2) can be written for constraints involving particle orientations, but we treat them differently. We simply determine the smallest rotational correction that satisfies the constraint, and apply it to rotate the corresponding layout object (see Sections 3.3.10 and 3.3.11).

### 3.2 Parenting and Grouping

Layout objects can be grouped; for example, tiers of seats in a theater, or a table and chairs. In our framework, the group is also represented by an oriented particle. The dimensions and size of the group is approximated by a bounding box. Furthermore, we can hierarchically define layout constraints within the group.

Constraints internal to a group can be rigid or nonrigid. In the rigid case, we simply apply positional corrections only to the particle representing the group, such that the grouped objects remain fixed relative to each other. In the nonrigid case, the particle representing the group can move, but so can the grouped objects with respect to one another subject to the layout constraints internal to the group.

For example, Fig. 4 illustrates objects grouped along line segments and circular arcs, which enables us to design seating tiers and add pathways in the theater scenes of Fig. 3

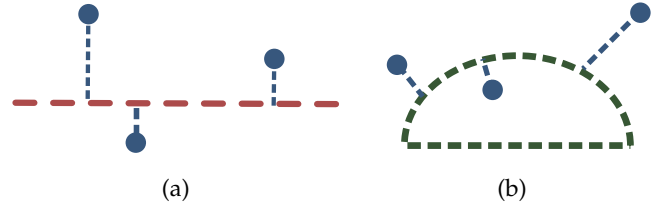


Fig. 4: Layout objects can be constrained relative to curves, such as line segments (a) or circular arcs (b), enabling the imposition of nonrigid group relationships.

while maintaining pairwise distances between the chairs. Segments are defined by the medial axis of the group’s bounding box. An arc is defined by its endpoints along with the center of the circle. When the particle representing the group moves, for each object in the group, a pairwise distance constraint (Section 3.3.1) is applied between a member object and the nearest point on the curve, which is represented by a particle with infinite mass. Since the curve is represented parametrically, the parametric ordering of the associated layout objects can be used to apply the pairwise distance and other group constraints, and the ordered application of constraints can improve convergence. We interleave the application of constraints, as proposed by Umetani et al. [31].

### 3.3 Constraint Types

The following sections discuss the constraints that we employ to produce layouts that are consistent with design standards [32].

#### 3.3.1 Pairwise Distance Constraint

In interior design, two furniture objects  $i$  and  $j$  (e.g., a chair and a table) are often required to be at a certain distance from each other in order for the layout to be deemed comfortable. We impose a desired distance  $d$  between the particles  $i$  and  $j$  representing the objects (Fig. 5a) with the constraint function

$$C(\mathbf{p}) = \|\mathbf{p}_{ij}\| - d, \quad (4)$$

where  $\mathbf{p}_{ij} = \mathbf{p}_i - \mathbf{p}_j$ , with gradients

$$\nabla_{\mathbf{p}_i} C(\mathbf{p}) = \hat{\mathbf{p}}_{ij}; \quad \nabla_{\mathbf{p}_j} C(\mathbf{p}) = -\hat{\mathbf{p}}_{ij}, \quad (5)$$

where  $\hat{\mathbf{p}}_{ij} = \mathbf{p}_{ij} / \|\mathbf{p}_{ij}\|$ . Imposed as an equality constraint  $C(\mathbf{p}) = 0$ , the particle positional corrections are [23]

$$\Delta \mathbf{p}_i = -\frac{w_i C(\mathbf{p})}{w_i + w_j} \hat{\mathbf{p}}_{ij}; \quad \Delta \mathbf{p}_j = \frac{w_j C(\mathbf{p})}{w_i + w_j} \hat{\mathbf{p}}_{ij}. \quad (6)$$

#### 3.3.2 Focal Point Distance Constraint

An object, such as the stage in a theater or a TV in a living-room, can be deemed a *focal point* for a group of objects [33], [34], and the objects may be constrained to be at a distance  $d$  from the focal point. We enforce such constraints simply by adding a pairwise distance constraint (4) between the particle  $\mathbf{p}_j$  that represents the focal point object and each of the surrounding objects represented by particles  $\mathbf{p}_i$  (Fig. 5b). The focal point object can be prevented from correcting its position by setting its inverse mass  $w_j$  to zero.

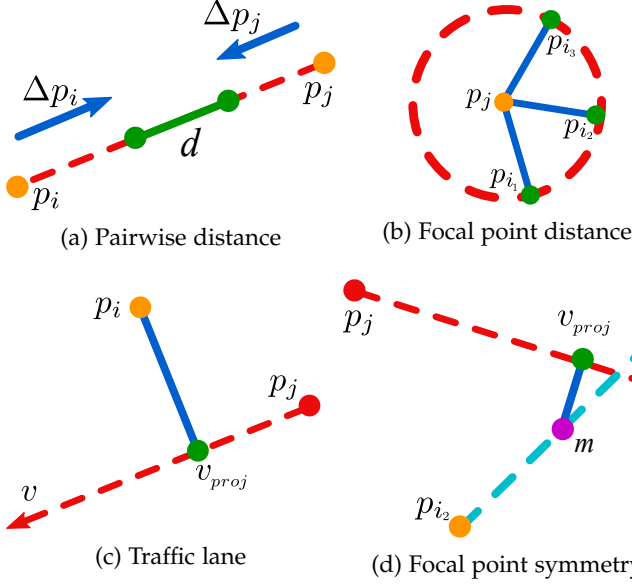


Fig. 5: Different positional layout constraints. Note that in (d),  $C$  denotes the center of mass of particles  $j_1$  and  $j_2$ .  $v_{proj}$  denotes the projection of  $C$  onto the vector starting at focal point  $i$ .

### 3.3.3 Traffic Lane Constraint

Objects should often be arranged to accommodate traffic lanes that introduce space between objects or groups of objects to allow easy access [33], [34]; e.g., walkways in a theater (Fig. 3). To this end, we enforce a clearance around a vector extending from a particle. This is implemented analogously to a pairwise distance constraint (4) between a particle  $p_i$  and the closest point  $p_{v_{proj}}$  on a vector  $v$  from another particle  $p_j$  (Fig. 5c):

$$C(\mathbf{p}) = \|\mathbf{p}_i - \mathbf{p}_{v_{proj}}\| - d, \quad (7)$$

where

$$\mathbf{p}_{v_{proj}} = \mathbf{p}_j + \frac{\mathbf{p}_{ij} \cdot \mathbf{v}}{\mathbf{v} \cdot \mathbf{v}} \mathbf{v}, \quad (8)$$

is the point along  $v$  nearest to  $p_i$ , and  $d$  is the desired minimal distance of  $p_i$  from  $v$ ; i.e., (7) is enforced as an inequality constraint,  $C(\mathbf{p}) \geq 0$ . We treat  $p_{v_{proj}}$  as a *ghost* particle that is rigidly attached to  $p_j$ . Hence, any positional correction of  $p_{v_{proj}}$  is applied to  $p_j$ . The ghost particle has inverse mass  $w_j$ , which may be set to 0 if need be to prevent the constraint from affecting the position of  $p_j$ .

### 3.3.4 Heat Point Constraint

For an object or group of  $n$  objects, the *heat point*  $\tilde{\mathbf{p}}$  is the position where the center of mass,  $\mathbf{m} = w \sum_{i=1}^n m_i \mathbf{p}_i$  with  $w = 1/m$  and  $m = \sum_{i=1}^n m_i$ , of the particles  $p_i$  representing the objects is required to be. For example, a computer display, keyboard, and mouse should be located near the middle of the front of a tabletop for easy access. To this end, we define the constraint function

$$C(\mathbf{p}) = \frac{1}{2} \|\mathbf{m} - \tilde{\mathbf{p}}\|^2, \quad (9)$$

whose gradient for particle  $p_j$  is

$$\nabla_{\mathbf{p}_j} C(\mathbf{p}) = m_j w (\mathbf{m} - \tilde{\mathbf{p}}). \quad (10)$$

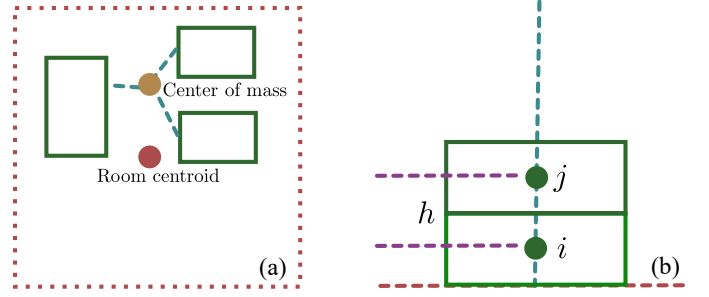


Fig. 6: (a) Visual balance. (b) Stacking constraint:  $h$  denotes the vertical distance between the centers of objects  $i$  and  $j$ .

### 3.3.5 Focal Point Symmetry Constraint

We can constrain a group of objects to be positioned symmetrically around a vector  $v$  directed away from the group’s focal point  $p_j$ —e.g., two chairs positioned symmetrically in front of the television—by projecting the center of mass  $\mathbf{m}$  of their representative particles onto  $v$  (Fig. 5d). We constrain  $\mathbf{m}$  to coincide with the projection  $p_{v_{proj}}$  using a constraint function analogous to (9):

$$C(\mathbf{p}) = \frac{1}{2} \|\mathbf{m} - \mathbf{p}_{v_{proj}}\|^2. \quad (11)$$

### 3.3.6 Visual Balance Constraint

Placing all the furnishings at one end of a room would create an imbalanced, inharmonious ambiance, which prompted Merrell *et al.* [4] to propose a visual balance constraint. To create a sense of equilibrium, we want to arrange the furnishings such that the mean of the visual weights is close to the center of the room [33], [35]. Since larger objects have more visual weight, we define the visual weight of an object in accordance to its dimensions projected onto the ground plane. We implement a visual balance constraint analogously to (9) between the room’s centroid  $c$  and the center of mass  $\mathbf{m}$  of particles representing the visual weights of furnishings (Fig. 6a):

$$C(\mathbf{p}) = \frac{1}{2} \|\mathbf{m} - c\|^2, \quad (12)$$

where  $c$  denotes the center of the room. Since the room’s centroid is static, particle  $c$  is assigned zero inverse mass.

### 3.3.7 Layout Boundaries and Distance to Wall Constraint

Large furnishings usually work best when placed near a wall [33]. For example, we usually avoid placing bookshelves in the center of a room. Also, in realistic use cases, furnishings should not collide with walls. Finally, all layout objects are constrained by layout boundaries.

We define both inequality and equality constraints for object  $i$  constrained to be near a wall with distance  $d$  (Fig. 7a) as follows:

$$C(\mathbf{p}) = \|\mathbf{p}_i - \mathbf{p}_{wall}\| - d, \quad (13)$$

where  $p_{wall}$  is the point on the wall nearest to the position  $p_i$  of the particle representing object  $i$  (in case of multiple nearest points, we simply choose the first point found). The positional corrections are analogous to (6), but note that since  $p_{wall}$  is fixed, corrections are applied only to  $p_i$ .

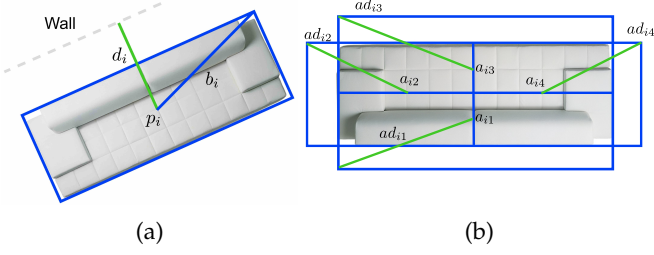


Fig. 7: (a) Wall distance and orientation constraint ( $\mathbf{p}_i$  denotes the center of object  $i$  and  $b_i$  is the size of its bounding box). (b)  $ad_{ik}$  denotes the accessibility distance of the respective accessibility center  $\mathbf{a}_{ik}$ .

### 3.3.8 Accessibility Constraint

Clearance between furniture items is essential for human comfort [33]. For instance, a coffee table should be close, but not too close, to a sofa in a living-room. We employ a modified version of an accessibility constraint proposed by Yu et al. [3]. Every object  $j$  is associated with a bounding box, where the faces of the bounding box that are orthogonal to the ground plane are identified with accessibility centers  $\mathbf{a}_{jk}$ , where  $k \in \{1, 2, 3, 4\}$  correspond to the back, left, front, and right faces, respectively.

Our accessibility constraint is defined using a pairwise distance constraint function between particle  $\mathbf{p}_i$  representing object  $i$  and  $\mathbf{a}_{jk}$ , accessibility center  $k$  of object  $j$  (Fig. 7b):

$$C(\mathbf{p}) = \|\mathbf{p}_i - \mathbf{a}_{jk}\| - d. \quad (14)$$

Distance  $d = b_i + ad_{jk}$ , where  $b_i$  is the diagonal of the bounding box of the object, and  $ad_{jk}$  is the diagonal of the accessibility center. The accessibility constraint is an inequality constraint  $C(\mathbf{p}) \geq 0$ , which is activated only if the respective cuboids defined by the accessibility distances intersect. The positional correction to  $\mathbf{p}_j$  is applied as if accessibility point  $\mathbf{a}_{jk}$  is rigidly attached.

### 3.3.9 Collision Constraint

The collision constraint is complementary to the accessibility constraint. Simply put, to ensure a realistic layout, the bounding cuboids of the layout objects should not collide. To that end, collisions between objects are resolved by a pairwise distance inequality constraint between the bounding spheres (Fig. 8a). Let  $\mathbf{p}_i$  and  $\mathbf{p}_j$  represent objects  $i$  and  $j$  whose bounding sphere radii are  $r_i$  and  $r_j$ . Our inequality collision constraint function is

$$C(\mathbf{p}) = \|\mathbf{p}_i - \mathbf{p}_j\| - (r_i + r_j). \quad (15)$$

Since checking for all pairwise object collisions is computationally expensive, we employ a spatial hash in order to reduce the number of collision checks.

If during the constraint projection objects  $i$  and  $j$  are colliding, and both are constrained to be next to a wall (Section 3.3.7), we perform an additional collision constraint projection between their respective closest wall points (Fig. 8b). These wall points are considered rigidly attached ghost particles. This allows us to satisfy both the pairwise distance constraint and the distance to wall constraint. If there are multiple candidate wall points, we simply choose the first one found.

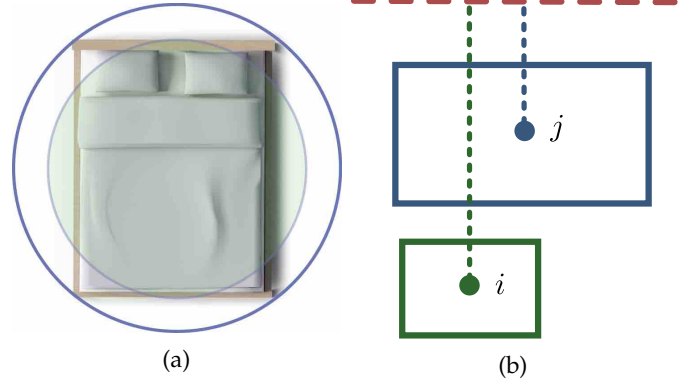


Fig. 8: (a) Our method resolves collisions between layout item's by resolving collisions between the respective bounding spheres. (b) Additional collision constraint between two layout items  $i$  and  $j$  that are also constrained to be next to the wall.

### 3.3.10 Pairwise Orientation Constraint

In layout design, the proper orientation of an object relative to another object in the same furnishing group can promote intimacy or improve functionality [36]. For example, a sofa should face a TV, a coffee table should be parallel to a sofa, and a seat in a theater should face the stage.

Yu et al. [3] propose a pairwise orientation constraint between interacting layout objects. Similarly, we define an equality orientation constraint between interacting particles  $i$  and  $j$ . Let  $\theta_i$  and  $\theta'_i$  be the current and desired orientation of particle  $i$  relative to  $\mathbf{p}_j$ , and let  $\theta_j$  and  $\theta'_j$  be the current and desired orientation of particle  $j$  relative to  $\mathbf{p}_i$ . Then the pairwise orientation constraint functions are defined as

$$C_i(\mathbf{p}) = |\theta_i - \theta'_i|; \quad C_j(\mathbf{p}) = |\theta_j - \theta'_j|, \quad (16)$$

where we calculate the smallest angular difference  $\Delta\theta_i$  between  $\theta_i$  and  $\theta'_i$ , and similarly for particle  $j$ . This rotational correction is then applied to the particles with corresponding stiffness  $k$ . The corrected particle orientations are  $\theta_i + k\Delta\theta_i$  and  $\theta_j + k\Delta\theta_j$ . The particle positions  $\mathbf{p}_i$  and  $\mathbf{p}_j$  remain unchanged.

### 3.3.11 Orientation to Wall Constraint

Some furnishings work best when placed parallel to a wall (e.g., a table or TV shelf [33]). Following Yu et al. [3], we formulate an equality constraint between particle  $i$  and the nearest wall using the constraint function

$$C(\mathbf{p}) = |\theta_i - \theta_{\text{wall}}|, \quad (17)$$

where  $\theta_i$  is the orientation of the represented object with respect to the closest wall point and  $\theta_{\text{wall}}$  is its desired orientation. To satisfy this constraint, we proceed analogously to the previous section.

### 3.3.12 Vertical Stacking Constraint

In layout design, accessories serve either a functional or decorative purpose [33]. Vertical stacking is a common way to arrange accessories. For example, books may be stacked in order to conserve space.

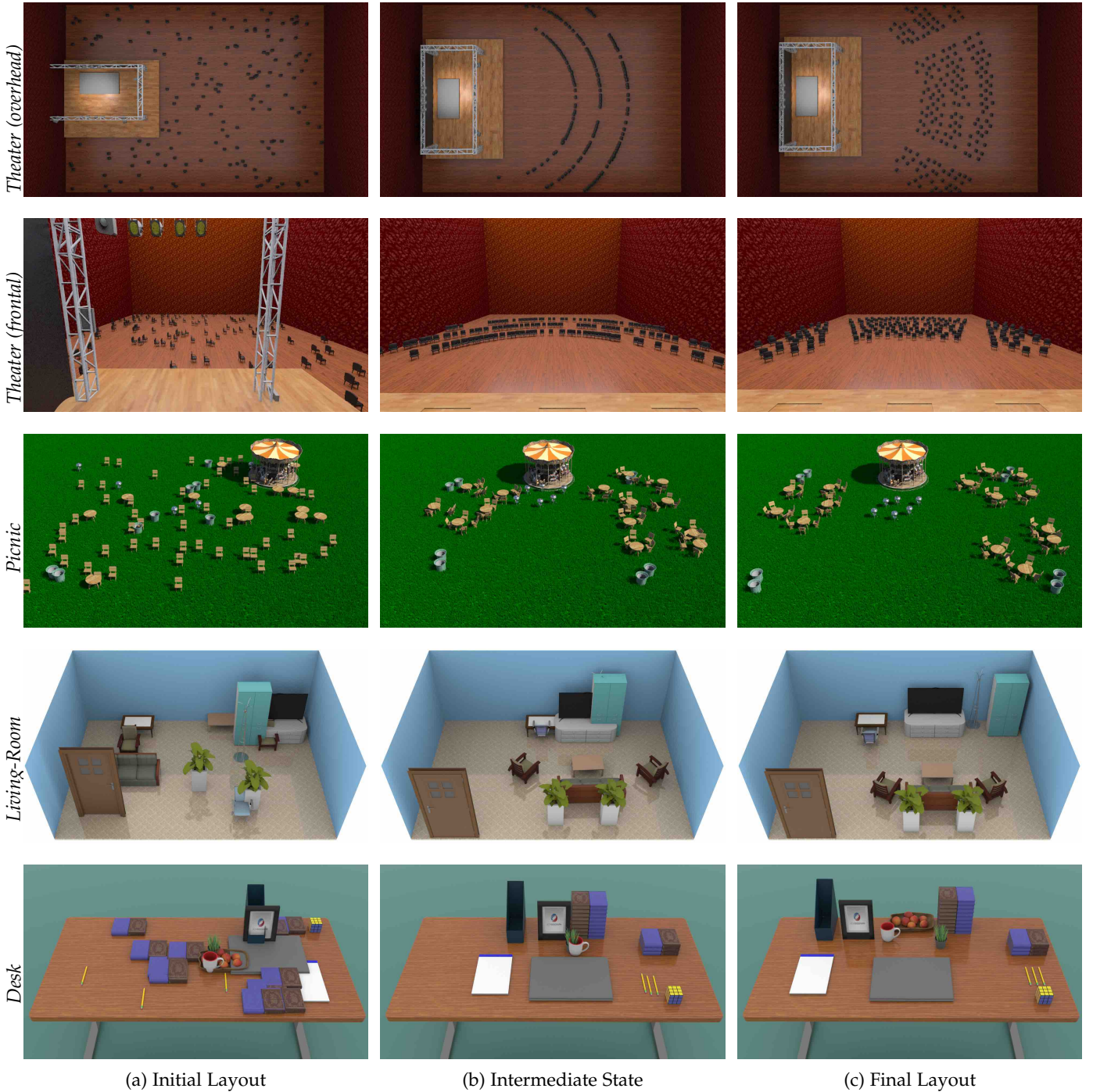


Fig. 9: Various synthesized layouts.

Objects to be stacked can be prespecified. If object  $j$  is to be stacked on object  $i$ , the vertical distance between the particles representing these objects should be equal to half the sum of the objects' heights  $h = (h_i + h_j)/2$ . We formulate the constraint function

$$C(\mathbf{p}) = z_j - (z_i + h), \quad (18)$$

involving the  $z$  components of  $\mathbf{p}_i$  and  $\mathbf{p}_j$ , with  $z$  axis normal to the ground plane. Hence, particle  $j$  should be placed above particle  $i$  (Fig. 6b). Additionally, we constrain the ground plane coordinates of particle  $j$  to match those of

particle  $i$ :

$$C(\mathbf{p}) = \|x_j - x_i\|; \quad C(\mathbf{p}) = \|y_j - y_i\|. \quad (19)$$

#### 4 EXPERIMENTS AND RESULTS

We implemented our layout synthesis system in Python and Cython, and ran our experiments on a 2.5 GHz Intel i7 Macintosh system.

Fig. 9 shows examples of our experimental scenarios. In each experiment, the initial object locations and orientations were set randomly, as shown in Fig. 9a. Accessibility and

**Theater-1 Constraints:**

Wall distance — stage  
 Distance — between each tier of seats and the stage  
 Traffic Lanes — between the seats and two vectors from the stage  
 Orientation — between the stage and each seat, which should face the stage  
 Focal point — for each seat in a seating tier, oriented toward the stage

**Theater-2 Constraints:**

Heat point — stage  
 Distance — between each tier of seats and the stage  
 Traffic Lanes — between all the seats and two vectors from the stage  
 Orientation — between the stage and each seat, which should face the stage  
 Grouping — between all the tiers  
 Grouping — between chairs in each seating tier

**Picnic Constraints:**

Focal point — each table is a focal point for a group of 4 chairs  
 Distance — between each chair in an associated group  
 Distance — the BBQ grills are linked together  
 Distance — between each pair of trash cans  
 Heat point — between each group of trash cans and a picnic layout location  
 Heat point — on each table to a different layout area  
 Heat point — on the Carousel to the top-middle corner of the layout  
 Orientation — between chairs and respective table

**Living-Room Constraints:**

Focal point — couch as focal point to table  
 Focal point — TV as focal point to couch, sofa chairs  
 Focal point — Table as focal point to office chair  
 Wall distance and orientation — TV, book case, coat rack, door, plants  
 Visual balance  
 Orientation — between objects and their respective focal points

**Desk Constraints:**

Stacking — between books, divided into two groups  
 Heat point — on laptop, to be located near the front middle of the desk.  
 Heat point — on notepad to front right of desk  
 Heat point — on Rubik’s cube to front left of desk  
 Distance — between potted plant and book stack  
 Distance — between book stack and desk binder  
 Distance — between binder and photo frame  
 Distance — between photo frame and mug  
 Distance — between pencils  
 Focal point — laptop as focal point to fruit plate  
 Focal point — Rubik’s cube as focal point to pencil group  
 Focal point — Rubik’s cube as a focal point to stack of books  
 Wall distance — on one stack of books

**Tightly-Packed Bedroom Constraints:**

Focal point — each table is a focal point for a group of 4 chairs  
 Distance — between floor lamp, table and chair  
 Distance — between chair and table  
 Distance — between bookcase and coat rack  
 Orientation — between chair and table  
 Wall distance — for beds, bookcase and table

**Tightly-Packed Picnic Constraints:**

Distance — the BBQ grills are linked together  
 Distance — between each pair of trash cans  
 Heat point — between each group of trash cans and a picnic layout location  
 Heat point — on the Carousel to the top-middle corner of the layout

Fig. 10: The constraints used in our experiments.

collision constraints apply and are generated in all experiments. We ran our layout synthesis algorithm with the constraints described below (refer to Fig. 10). Since collision, accessibility, and wall constraints are treated as hard constraints, for weights in the energy function (1) we chose 150.0 for the collision and accessibility constraints, 20.0 for the wall constraints, and 1.0 for the remaining constraints. We determined these to be suitable weights experimentally. The iterative procedure terminates when there has been no improvement to the minimum layout energy for the previous 50 iterations.

Table 1 reports the run-times of our experiments. As shown in Fig. 11, most of the computation time is expended in solving the accessibility and collision constraints,

## 4.1 Layout Synthesis

We next describe the experimental scenarios of Fig. 9.

	# Objects	Our Method (sec)	SA-McMC (sec)
Theater-1	201	39.50	5852
Theater-2 (arc-0)	181	1.27	$\infty$
Theater-2 (arc-1)	181	1.31	$\infty$
Theater-2 (arc-2)	181	1.36	$\infty$
Theater-2 (seg-0)	169	0.48	$\infty$
Theater-2 (seg-1)	169	0.52	$\infty$
Theater-2 (seg-2)	246	0.73	$\infty$
Picnic	77	4.77	253
Living-Room	10	0.62	27
Desk	21	0.69	37
TP Bedroom	12	0.67	22
TP Picnic	53	2.42	109

TABLE 1: Comparing the run-times of our method versus the baseline SA-McMC method. Times shown are the mean of 10 runs with the same starting conditions for both methods. TP denotes “tightly-packed”. For the Theater-2 scene, {arc,seg}-# denotes the number of pathways. Collision detection is disabled in Theater-2. For Theater-2, we failed to achieve reasonable synthesis results in finite time with our SA-McMC implementation; better-designed SA-McMC shift moves may help.

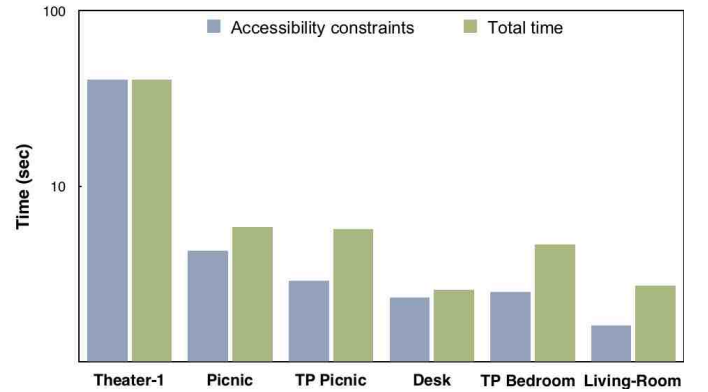


Fig. 11: Run-times of our method. TP denotes “tightly-packed”. The major computational cost stems from resolving the accessibility and collision constraints, especially when increasing the number of layout objects.

### 4.1.1 Theater Variations

We demonstrated the efficacy of our method by running our algorithm in a theater scene with various seating arrangements and two different constraint strategies:

- 1) Each chair is at a predefined distance to the stage due to a focal point constraint, and is constrained not to collide with other chairs. The chairs are not associated with tiers, and there are no pairwise distance constraints between chairs in the same tier (Fig. 9).
- 2) Each chair is part of a seating tier that is either a segment or an arc group. Each particle is constrained to have the same distance from neighboring particles in the tier. Tiers are constrained to be centered before the stage (Fig. 3), or layouts like that in Fig. 12 may result.

The stage is initially located at the front midpoint of the theater. There are up to 2 traffic lanes for stage pathways.

With Approach 1, we allocated 200 chairs and further tested the scalability of our algorithm by running additional experiments with varying numbers of chairs. Fig. 13 plots the run-times. Distances are enforced through accessibility and collision constraints; even without distance constraints, the chairs maintain nearly regular intra-tier distributions.



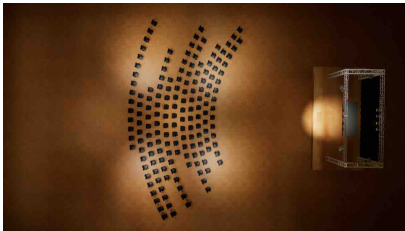


Fig. 12: Theater with tiers not restricted to front of stage.

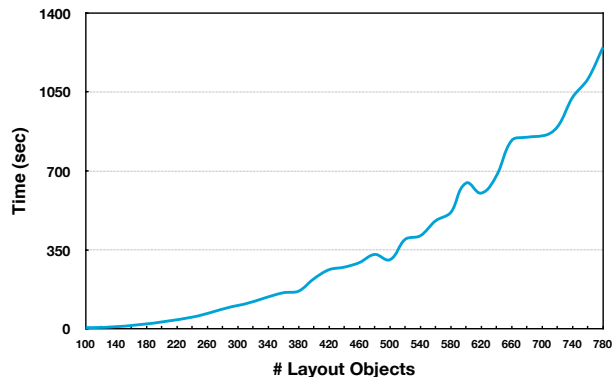


Fig. 13: Run-times for increasing numbers of theater seats in the Theater-1 scenario.

The scenes synthesized with Approach 2 involve between 168 to 246 layout objects. Within tiers, the distribution of chairs is constrained to be around the center of the tier, using a heat point constraint. The traffic lanes conflict with the pairwise distance constraints of the chairs in each tier.

#### 4.1.2 Picnic

The picnic scene consists of 14 tables, 48 chairs, 8 trash cans, 6 BBQ grills, and a carousel. The main constraints are focal point constraints between each group of chairs and their table, distances between chairs around tables, distances between tables, and heat point constraints to position BBQ grills, trash cans, and picnic tables.

#### 4.1.3 Living-Room

The living-room layout (Fig. 14) contains 2 chairs, 2 indoor plants, a sofa and armchairs, a coat rack, a door, a desk, an office chair, and a TV. The main constraints are focal point constraints between the TV, sofa, and armchairs, as well as wall constraints on the big furniture objects and plants.

#### 4.1.4 Desk

We also demonstrated the performance of our algorithm for a desk with small objects, including 12 books, 3 pencils, a food plate, a binder, a photo frame, a potted plant, a laptop computer, and a mug. The main constraints are focal point constraints between certain objects, heat point constraints on different desk parts, and a stacking constraint for the books.

## 4.2 Layout Synthesis in Tightly-Packed Scenarios

Our method copes well with highly constrained and tightly-packed settings.



Fig. 14: Optimized living room layout satisfying criteria such as distance, viewing angle, focal point grouping, and visual balance, starting from the initial random layout shown beneath.

#### 4.2.1 Tightly-Packed Bedroom

The tightly packed bedroom contains multiple beds and pieces of furniture. The beds are rigidly grouped together with army style accessories. The beds, bookcase and table are constrained to be next to the wall. The coat rack is constrained to be at a certain distance from the bookcase. We demonstrate that using different initial conditions results in different suggested layouts. Even though the space is tight, our method successfully synthesizes different layout suggestions (Fig. 15).

#### 4.2.2 Tightly-Packed Picnic

This tightly-packed setting demonstrates our method's ability to synthesize diverse layouts with different numbers and types of furniture objects. We synthesize a tightly-packed picnic scenario in two stages. In the first stage, we randomly vary the number of layout objects of each type, similar to Yeh *et al.* [5]. The available layout objects are a superset of the previous picnic scenario, with an additional rectangular picnic table. For a more uniform layout, we rigidly attached 4 chairs to each round picnic table. In the second stage of the synthesis, we run our method for 270 iterations. Fig. 2 shows these synthesized layouts.

## 4.3 Comparison to Simulated Annealing

We compared the performance of our method to a baseline layout synthesis approach that applies simulated annealing with a Metropolis-Hastings MCMC state-search step, which we denote SA-MCMC. Our implementation is based on code used in [3]. In this implementation, the proposal function shifts an attribute of one layout object in each state-search step. We employed the same energy function (1) to track the quality of the synthesized layouts and ran the comparison several times, with different conditions, such as varying constraint weights  $\gamma_i$  and temperature schedules for the

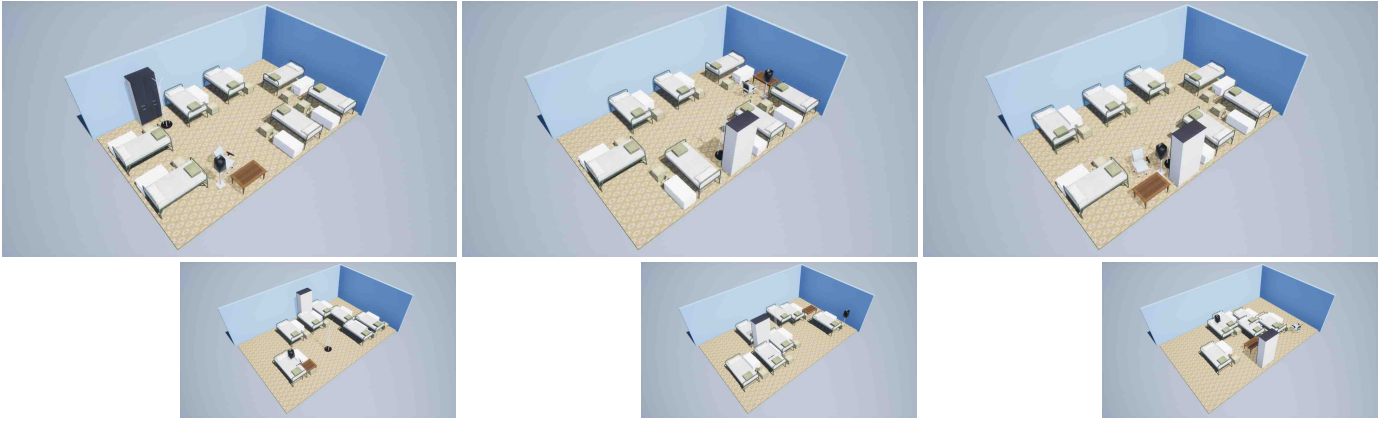


Fig. 15: Different layout suggestions (top) synthesized by initializing from different random initial conditions (bottom).

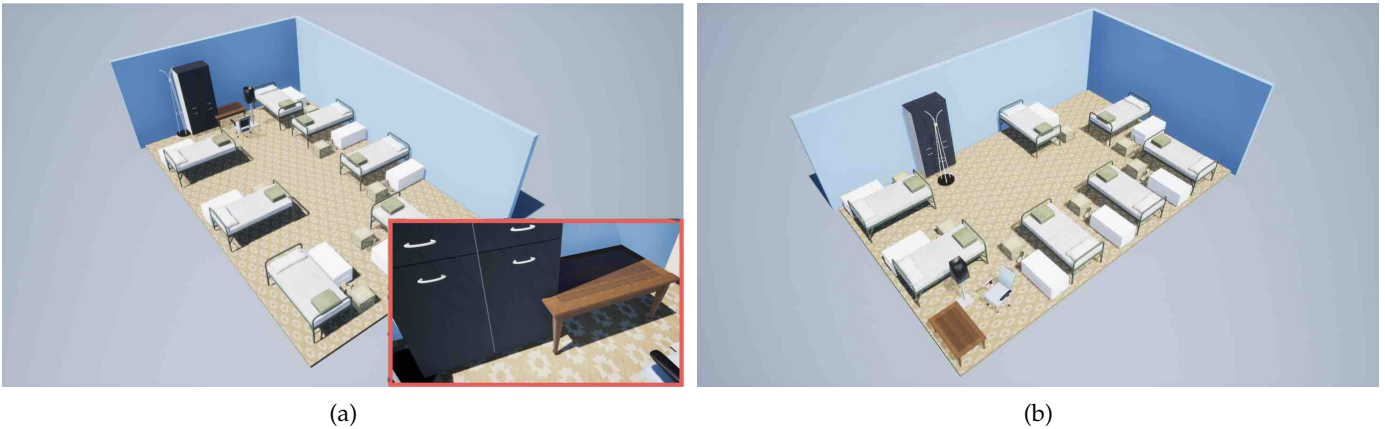


Fig. 16: (a) A baseline SA-McMC approach struggles with a tightly-packed bedroom. Using stochastically sampled shift moves results in objects becoming “locked” in configurations that are probabilistically hard to escape. (b) Our method does not. Since the table, rack and closet are colliding and constrained to be next to the wall, the objects manage to escape this configuration following a positional correction that enforces collision and distance to wall constraints. See Section 3.3.9.

SA-McMC algorithm. For all our experiments, we used linear, evenly-spaced schedules for about 20,000 iterations, with an additional stopping condition in case the energy function value did not improve by more than 0.1% during the previous 1,500 iterations.

Experimentally, we noticed that a baseline SA-McMC approach has trouble accommodating tightly-packed and constrained layouts, as in the tightly-packed bedroom and picnic scenarios described in the previous section. Superficially, synthesized layouts appeared satisfactory; however, upon closer inspection, they suffered from unresolved collisions (Fig. 16a). A possible explanation is that, unlike our approach, SA-McMC does not exploit local constraint gradient information when shifting between layout configurations. In theory, SA-McMC can escape such collisions through the choice of different parameter settings, using more complex hand-crafted SA-McMC shifts moves, and/or tuning the weights of different constraints in the energy. Unfortunately, none of the settings with which we experimented yielded collision-free layout suggestions for the tightly-packed scenarios.

Fig. 17 plots the energy as a function of iteration number for SA-McMC and our method for the tightly-packed picnic scenario shown in Fig. 1. Generally, we observed that SA-

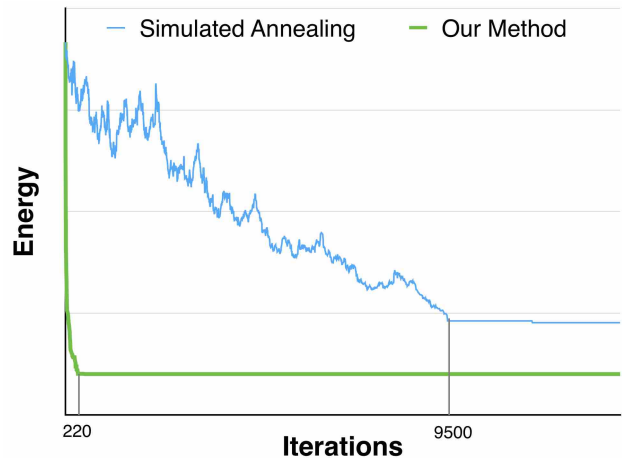


Fig. 17: Energy plot (linear scale) of our method versus SA-McMC [3] for the tightly packed picnic layout. The total run-time for SA-McMC was approximately 163 seconds, versus 4.7 seconds for our method. Our method converged to a satisfactory layout at around iteration 220. SA-McMC converged to a less satisfactory, higher-energy layout after 9,500 iterations.

McMC is slower by at least an order of magnitude compared to our method (Table 1). The computational cost of SA-McMC increases dramatically with the number of objects to be synthesized. Hence, our method is the one that is more suitable for interactive applications.

## 5 DISCUSSION

We have demonstrated that continuous, deterministic, point-based simulation methods can produce satisfactory layout synthesis results at low computational cost, at least an order of magnitude faster than previous methods, which makes it suitable for augmented reality applications (Appendix A). Layout synthesis objectives are represented by a set of positional and orientational constraints. Our approach satisfies the conflicting set of constraints iteratively, resulting in fast layout synthesis with quality similar to or better than that of previous stochastic, McMC-based alternatives.

Previous work in layout synthesis does not incorporate constraint gradient information, but instead uses manually crafted McMC moves that augment a layout configuration. While this type of method provides an easy mechanism to explore different layout variations, we achieve the same effect via different initializations. As observed in our comparison, the run-times of the baseline SA-McMC method increases significantly with the number of layout objects. In these approaches, a user can define a more relaxed set of constraints, which at least in principle could lead to a desired layout, but at much greater computational cost. In practice, we observed that these methods perform poorly in tightly-packed layouts, resulting in unrealistic collisions between layout items. By contrast, our method is dramatically faster due to its continuous nature. Notably, it requires only a few seconds of run-time for dozens of objects and it naturally scales to hundreds of objects with only moderately increasing computational cost.

Since layout synthesis poses a non-convex problem, it is difficult—and fortunately unnecessary—to find the global optimum. We experimented with nonlinear global optimization solvers (NLOpt [37]), but the results were either poor in quality (i.e., unrealistic layouts with many colliding layout items), or the run-times were intractable. In contrast to these solvers, our method does not directly try to minimize the global energy, but rather iteratively satisfies individual constraints. This induces positional corrections to layout items that propagate throughout the layout, transforming an initially poor, high-energy layout to a satisfactory low-energy layout. The global energy quantifies the quality of layouts and enables our comparisons to prior work.

The intended workflow of layout synthesis methods is for the automated approach to synthesize a variety of viable layouts, from which the user can select one or more that they prefer. Our method supports this workflow. It can generate a variety of layouts by repeatedly running from different random initial conditions (Fig. 15). Ultimately, the quality of configurations is a subjective matter. Hence, at least from the user’s perspective, a global optimum is not definitive.

### 5.1 Limitations

We observed that solving constraints sequentially, where the new positions are immediately visible to other constraints,

makes quick progress at first, but the convergence rate slowly decreases as the iterations progress. For example, in the living-room experiment, the first few iterations yield a layout that is visually similar to the final one, whereas later iterations produce smaller refinements of the layout and resolve cuboid accessibility area intersections.

Like SA-McMC, the layout’s energy can increase from one iteration to the next, which allows to escape suboptimal local minima. Unlike SA-McMC, our method may not converge in the traditional optimization sense; however, our termination criterion is based on the satisfaction of most of the constraints, which is ultimately what matters. In practice, we never observed outcomes that failed to satisfy layout objectives. Most starting seeds lead to a satisfactory layout, all lead to a collision free layout. Although conceptually simple, our method produces impressive results.

### 5.2 Future Work

In the present study, we did not encode all the constraints that may be relevant in layout design; however, our method can easily be extended to a broader set of layout constraints. Incorporating GPU parallelization can further speed up the procedure, as could a hierarchical approach, where the layout synthesis problem is broken into stages. It will also be interesting to adjust the stiffness factors in a nonuniform manner in an effort to converge to better global solutions.

Due to the sequential, local constraint satisfaction approach of our position-based method, we may observe oscillations and collisions between objects. For example, when there is a collision between the accessibility areas of two objects, the constraint may be partially resolved by projecting one of these objects into a collision with a third object. In future work, we plan to design automatic schemes for detecting and resolving these conditions.

The layout objects and their relationship to their corresponding groups can be stochastically sampled from predefined distributions; e.g., from real-world scene datasets. This is similar to but faster than applying factor graphs [5].

## APPENDIX A AUGMENTED REALITY LAYOUT SYNTHESIS

As another use-case example of our method, we demonstrate the fast synthesis of furniture layouts from and into 2D images of vacant spaces. After the user uploads an image of an indoor or outdoor space, selects furnishings, and specifies layout objectives, our system then automatically analyzes the space using scene understanding algorithms from computer vision, and finally renders into the original image optimal layouts of the selected furnishings satisfying the given objectives. The system works as follows:

- 1) Semantic scene segmentation: Our system employs SegNet [38], a state-of-the-art, pixel-wise semantic segmentation network, trained on the SUN-RGBD dataset [39] with common indoor scene objects, to output 37 categories of per-pixel semantic image labels. GrabCut [40] is then applied to segment the pixels labeled ‘floor’. Fig. 18 shows examples of the segmentation.
- 2) 3D scene estimation: We ask users to place a checkerboard calibration marker into the imaged scene, from

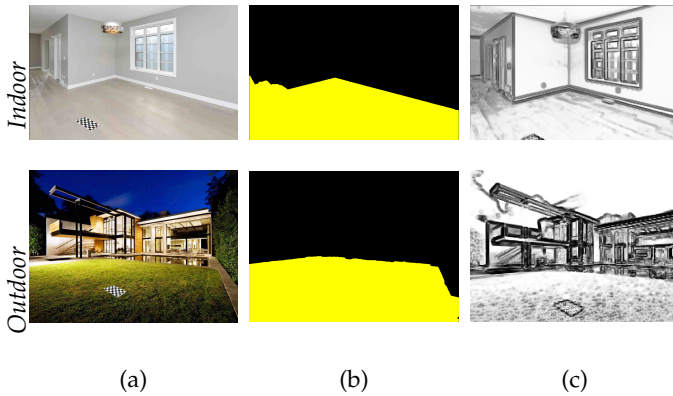


Fig. 18: Segmentation and edge detection. (a) Original images. (b) Segmented floor/ground. (c) Edge maps.

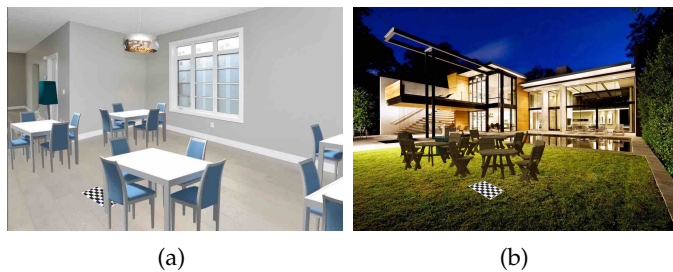


Fig. 19: Synthesized results from user-provided images. (a) Synthesized indoor layout. (b) Synthesized outdoor layout.

which our system estimates the camera parameters, the orientation and scale of the floor/ground, and (using Holistically-Nested Edge detection [41]) the height of the scene perpendicular to the estimated ground plane.

- Layout synthesis and visualization: The system runs our layout synthesis method to generate optimal layouts, which it then renders into the image via a virtual camera with the aforementioned estimated camera parameters. Fig. 19 shows examples of the results.

Reference [42] provides additional details.

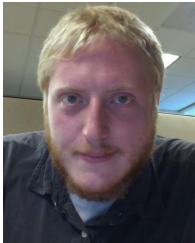
## REFERENCES

- R. M. Smelik, T. Tutenel, R. Bidarra, and B. Benes, "A survey on procedural modelling for virtual worlds," in *Comp. Graphics Forum*, vol. 33, no. 6, 2014, pp. 31–50.
- S. Chib and E. Greenberg, "Understanding the Metropolis-Hastings algorithm," *The American Statistician*, vol. 49, no. 4, pp. 327–335, 1995.
- L.-F. Yu, S. K. Yeung, C.-K. Tang, D. Terzopoulos, T. F. Chan, and S. Osher, "Make it home: Automatic optimization of furniture arrangement," *ACM Trans. Graphics*, vol. 30, no. 4, p. 86, 2011.
- P. Merrell, E. Schkufza, Z. Li, M. Agrawala, and V. Koltun, "Interactive furniture layout using interior design guidelines," in *ACM Trans. Graphics*, vol. 30, no. 4, 2011, p. 87.
- Y.-T. Yeh, L. Yang, M. Watson, N. D. Goodman, and P. Hanrahan, "Synthesizing open worlds with constraints using locally annealed reversible jump MCMC," *ACM Trans. Graphics*, vol. 31, no. 4, p. 56, 2012.
- Q. Fu, X. Chen, X. Wang, S. Wen, B. Zhou, and H. Fu, "Adaptive synthesis of indoor scenes via activity-associated object relation graphs," *ACM Trans. Graphics*, vol. 36, no. 6, p. 201, 2017.
- T. Feng, L.-F. Yu, S.-K. Yeung, K. Yin, and K. Zhou, "Crowd-driven mid-scale layout design," *ACM Trans. Graphics*, vol. 35, no. 4, 2016.
- M. Fisher, D. Ritchie, M. Savva, T. Funkhouser, and P. Hanrahan, "Example-based synthesis of 3D object arrangements," *ACM Trans. Graphics*, vol. 31, no. 6, p. 135, 2012.
- C.-H. Peng, Y.-L. Yang, and P. Wonka, "Computing layouts with deformable templates," *ACM Trans. Graphics*, vol. 33, no. 4, p. 99, 2014.
- W. Wu, L. Fan, L. Liu, and P. Wonka, "Miqp-based layout design for building interiors," in *Comp. Graphics Forum*, 2018.
- L. Majerowicz, A. Shamir, A. Sheffer, and H. H. Hoos, "Filling your shelves: Synthesizing diverse style-preserving artifact arrangements," *IEEE Trans. on Visualization and Comp. Graphics*, vol. 20, no. 11, pp. 1507–1518, 2014.
- F. Bao, D.-M. Yan, N. J. Mitra, and P. Wonka, "Generating and exploring good building layouts," *ACM Trans. Graphics*, vol. 32, no. 4, 2013.
- L. Zhu, W. Xu, J. Snyder, Y. Liu, G. Wang, and B. Guo, "Motion-guided mechanical toy modeling," *ACM Trans. Graphics*, vol. 31, no. 6, p. 127, 2012.
- Y. Cao, A. B. Chan, and R. W. Lau, "Automatic stylistic manga layout," *ACM Trans. Graphics*, vol. 31, no. 6, p. 141, 2012.
- Y. Cao, R. W. Lau, and A. B. Chan, "Look over here: Attention-directing composition of manga elements," *ACM Trans. Graphics*, vol. 33, no. 4, p. 94, 2014.
- B. Reinert, T. Ritschel, and H.-P. Seidel, "Interactive by-example design of artistic packing layouts," *ACM Trans. Graphics*, vol. 32, no. 6, p. 218, 2013.
- D. Terzopoulos, J. Platt, A. Barr, and K. Fleischer, "Elastically deformable models," *ACM Trans. Graphics*, vol. 21, no. 4, pp. 205–214, 1987.
- P.-L. Manteaux, C. Wojtan, R. Narain, S. Redon, F. Faure, and M.-P. Cani, "Adaptive physically based models in computer graphics," in *Comp. Graphics Forum*, 2016.
- H. Qin and D. Terzopoulos, "D-nurbs: a physics-based framework for geometric design," *IEEE Trans. on Visualization and Comp. Graphics*, vol. 2, no. 1, pp. 85–96, 1996.
- R. Attar, R. Aish, J. Stam, D. Brinsmead, A. Tessier, M. Glueck, and A. Khan, "Physics-based generative design," in *CAAD Futures Conf.*, 2009, pp. 231–244.
- M. Harada, A. Witkin, and D. Baraff, "Interactive physically-based manipulation of discrete/continuous models," *ACM Trans. Graphics*, pp. 199–208, 1995.
- S. A. Arvin and D. H. House, "Modeling architectural design objectives in physically based space planning," *Automation in Construction*, vol. 11, no. 2, pp. 213–225, 2002.
- M. Müller, B. Heidelberger, M. Hennix, and J. Ratcliff, "Position based dynamics," *Virtual Reality Interactions and Physical Simulations (VRIPHYS)*, vol. 18, no. 2, pp. 109–118, 2007.
- J. Stam, "Nucleus: Towards a unified dynamics solver for computer graphics," in *Proc. IEEE Int. Conf. on Comp.-Aided Design and Comp. Graphics*, 2009, pp. 1–11.
- C. Deul, P. Charrier, and J. Bender, "Position-based rigid-body dynamics," *Comp. Animation and Virtual Worlds*, vol. 27, no. 2, pp. 103–112, 2016.
- M. Macklin and M. Müller, "Position based fluids," *ACM Trans. Graphics*, vol. 32, no. 4, p. 104, 2013.
- T. Weiss, A. Litteneker, C. Jiang, and D. Terzopoulos, "Position-based multi-agent dynamics for real-time crowd simulation," in *Motion in Games*, ser. MIG '17. ACM, 2017, pp. 10:1–10:8.
- J. Bender, M. Müller, M. A. Otaduy, M. Teschner, and M. Macklin, "A survey on position-based simulation methods in computer graphics," in *Comp. Graphics Forum*, vol. 33, no. 6, 2014, pp. 228–251.
- E. L. Algower and K. Georg, *Introduction to Numerical Continuation Methods*. SIAM, 2003, vol. 45.
- M. Macklin, M. Müller, N. Chentanez, and T. Kim, "Unified particle physics for real-time applications," *ACM Trans Graph*, vol. 33, no. 4, p. 104, 2014.
- N. Umetani, R. Schmidt, and J. Stam, "Position-based elastic rods," in *Proc. of the ACM SIGGRAPH/Eurographics Symp. on Comp. Animation*, 2014, pp. 21–30.
- J. DeChiara, J. Panero, and M. Zelnic, *Time-Saver Standards for Interior Design and Space Planning*. McGraw-Hill, 2001.
- L. M. Jones and P. S. Allen, *Beginnings of Interior Environments*. Pearson, 2014.
- C. Deasy and T. E. Lasswell, *Designing Places for People*. Whitney, 1990.
- S. Lok, S. Feiner, and G. Ngai, "Evaluation of visual balance for automated layout," in *Proc. of the 9th Int. Conf. on Intelligent user interfaces*, 2004, pp. 101–108.

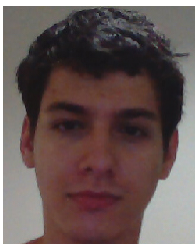
- [36] C. Talbot, M. Matthews, and C. Cosentino, *Decorating for Good: A Step-by-step Guide to Rearranging What You Already Own*. C. Potter, 1999.
- [37] S. G. Johnson, *The NLOpt nonlinear-optimization package*, 2011. [Online]. Available: <http://ab-initio.mit.edu/nlopt>
- [38] V. Badrinarayanan, A. Kendall, and R. Cipolla, "Segnet: A deep convolutional encoder-decoder architecture for image segmentation," *arXiv preprint arXiv:1511.00561*, 2015.
- [39] J. Xiao, J. Hays, K. A. Ehinger, A. Oliva, and A. Torralba, "Sun database: Large-scale scene recognition from abbey to zoo," in *Comp. Vis. and Pattern Recognition (CVPR)*, 2010, pp. 3485–3492.
- [40] C. Rother, V. Kolmogorov, and A. Blake, "Grabcut: Interactive foreground extraction using iterated graph cuts," *ACM Trans. Graphics*, vol. 23, no. 3, pp. 309–314, 2004.
- [41] S. Xie and Z. Tu, "Holistically-nested edge detection," in *Proc. of the Int. Conf. on Comp. Vis. (ICCV)*, 2015, pp. 1395–1403.
- [42] T. Weiss, M. Nakada, and D. Terzopoulos, "Automated layout synthesis and visualization from images of interior or exterior spaces," in *IEEE CVPR Workshop on Vis. Meets Cognition*, 2017, pp. 41–47.



**Tomer Weiss** received his PhD degree in computer science at the University of California, Los Angeles, in 2018 and his BSc degree in Computer Science from Tel Aviv University in 2013. Currently, he is an operations research engineer at Wayfair, Inc., and a research scientist in the UCLA Computer Graphics & Vision Laboratory. His research interests include computer graphics and optimization methods.



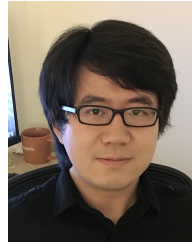
**Alan Littenecker** is a PhD student at the University of California, Los Angeles, and a member of the UCLA Computer Graphics & Vision Laboratory. He received his BSc degree in computer science from Chapman University in 2013. His research interests include computer graphics and cinematography.



**Noah Duncan** is Co-Founder and Chief Technology Officer at WorkPatterns, Inc. He received his PhD degree in computer science from the University of California, Los Angeles, in 2017 and his BSc degree in computer science from Harvey Mudd College in 2012. His research interests include computer graphics, with a focus on open-ended design problems.



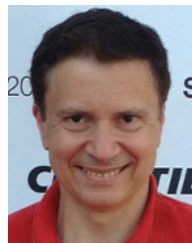
**Masaki Nakada** is a postdoctoral scholar in the UCLA Computer Graphics & Vision Laboratory. He obtained his PhD degree in computer science from the University of California, Los Angeles, in 2017 and his MS and BSc degrees in Applied Physics from Waseda University in Tokyo, Japan. His main research interests span machine learning, neuroscience, computer vision, computer graphics, and biomechanics.



**Chenfanfu Jiang** is an assistant professor of Computer and Information Science at the University of Pennsylvania. He received his PhD degree in Computer Science from the University of California, Los Angeles, in 2015 and was awarded the 2015 UCLA Henry Samueli School of Engineering and Applied Science Edward K. Rice Outstanding Doctoral Student Award. He received his BS degree in Physics in the Class for the Gifted Young (SCGY) of the University of Science and Technology of China (USTC) in 2010. His primary research focus is physics-based simulation and visual computing, and their overlap with computer vision, robotics, cognitive science, and medicine.



**Lap-Fai (Craig) Yu** is an assistant professor at the University of Massachusetts Boston, where he directs the Graphics and Virtual Environment Laboratory. He received his BEng and MPhil degrees in computer science from the Hong Kong University of Science and Technology (HKUST) in 2007 and 2009, respectively, and his PhD degree in computer science from the University of California, Los Angeles, in 2013, where he received the Cisco Outstanding Graduate Research Award. He is also a recipient of the Award of Excellence from Microsoft Research Asia. He has been a visiting scholar at Stanford University and a visiting scientist at the Massachusetts Institute of Technology. His research interests include computer graphics, computer vision, and virtual reality.



**Demetri Terzopoulos** is a Chancellor's Professor of Computer Science at the University of California, Los Angeles, where he holds the rank of Distinguished Professor and directs the UCLA Computer Graphics & Vision Laboratory. He is also Co-Founder and Chief Scientist of Voxel-Cloud, Inc. He graduated from McGill University and received his PhD degree ('84) in artificial intelligence from MIT. He is or was a Guggenheim Fellow, a Fellow of the ACM, a Fellow of the IEEE, a Fellow of the Royal Society of London, a Fellow of the Royal Society of Canada, a member of the European Academy of Sciences and the New York Academy of Sciences, and a life member of Sigma Xi. His many awards include an Academy Award for Technical Achievement from the Academy of Motion Picture Arts and Sciences for his pioneering work on physics-based computer animation, and the inaugural Computer Vision Distinguished Researcher Award from the IEEE for his pioneering and sustained research on deformable models and their applications. ISI and other indexes list him among the most highly-cited authors in engineering and computer science, with more than 400 published research papers and several volumes, primarily in computer graphics, computer vision, medical imaging, computer-aided design, and artificial intelligence/life. He has given hundreds of invited talks around the world about his research, including more than 100 distinguished lectures and keynote/plenary addresses. He joined UCLA in 2005 from New York University, where he held the Henry and Lucy Moses Professorship in Science and was Professor of Computer Science and Mathematics at NYU's Courant Institute of Mathematical Sciences. Previously, he was Professor of Computer Science and Professor of Electrical & Computer Engineering at the University of Toronto. Before becoming an academic in 1989, he was a Program Leader at Schlumberger corporate research centers in California and Texas.